Nephrol Dial Transplant (2012) 27: 1330–1343
doi: 10.1093/ndt/gfr483
Advance Access publication 5 September 2011

Albumin-induced apoptosis of glomerular parietal epithelial cells is modulated by extracellular signal-regulated kinase 1/2

Alice M. Chang[1], Takamoto Ohse[2], Ron D. Krofft[1], Jimmy S. Wu[1], Allison A. Eddy[3], Jeffrey W. Pippin[1] and Stuart J. Shankland[1]

[1]Division of Nephrology, University of Washington, Seattle, WA, USA, [2]Division of Nephrology and Endocrinology, University of Tokyo, Tokyo, Japan and [3]Division of Pediatric Nephrology, Seattle Children's Hospital and Research Institute, Seattle, WA, USA

Correspondence and offprint requests to: Alice M. Chang; E-mail: alice508@uw.edu

Abstract

Background. The biological role(s) of glomerular parietal epithelial cells (PECs) is not fully understood in health or disease. Given its location, PECs are constantly exposed to low levels of filtered albumin, which is increased in nephrotic states. We tested the hypothesis that PECs internalize albumin and increased uptake results in apoptosis.

© The Author 2011. Published by Oxford University Press on behalf of ERA-EDTA. All rights reserved.
For Permissions, please e-mail: journals.permissions@oup.com

Methods. Confocal microscopy of immunofluorescent staining and immunohistochemistry were used to demonstrate albumin internalization in PECs and to quantitate albumin uptake in normal mice and rats as well as experimental models of membranous nephropathy, minimal change disease/focal segmental glomerulosclerosis and protein overload nephropathy. Fluorescence-activated cell sorting analysis was performed on immortalized cultured PECs exposed to fluorescein isothiocyanate (FITC)-labeled albumin in the presence of an endosomal inhibitor or vehicle. Apoptosis was measured by Hoechst staining in cultured PECs exposed to bovine serum albumin. Levels of phosphorylated extracellular signal-regulated kinase 1 and 2 (p-ERK1/2) were restored by retroviral infection of mitogen-activated protein kinase (MEK) 1/2 and reduced by U0126 in PECs exposed to high albumin levels in culture and apoptosis measured by Hoechst staining.

Results. PECs internalized albumin normally, and this was markedly increased in all of the experimental disease models ($P < 0.05$ versus controls). Cultured immortalized PECs also internalize FITC-labeled albumin, which was reduced by endosomal inhibition. A consequence of increased albumin internalization was PEC apoptosis *in vitro* and *in vivo*. Candidate signaling pathways underlying these events were examined. Data showed markedly reduced levels of phosphorylated extracellular signal-regulated kinase 1 and 2 (ERK1/2) in PECs exposed to high albumin levels in nephropathy and in culture. A role for ERK1/2 in limiting albumin-induced apoptosis was shown by restoring p-ERK1/2 by retroviral infection, which reduced apoptosis in cultured PECs, while a forced decrease of p-ERK1/2 through inhibition of MEK 1/2 significantly increased albumin-induced PEC apoptosis.

Conclusions. A normal role of PECs is to take up filtered albumin. However, this is increased in proteinuric glomerular diseases, leading to apoptosis through changes in ERK1/2.

Keywords: albumin; apoptosis; glomerular parietal epithelial cell; glomerulosclerosis; proteinuria

Introduction

While major research and clinical strides have been made with glomerular endothelial cells, mesangial cells and podocytes in health and disease, glomerular parietal epithelial cells (PECs) remain the least understood of the four resident glomerular cell types. PECs and podocytes share a common embryological cell lineage [1]. However, each cell type begins to express different protein markers by the late S-shaped body phase of glomerulogenesis. While podocytes are terminally differentiated, mature PECs are not, and maintain low levels of proliferation under non-diseased conditions [2, 3]. Moreover, following certain forms of injury such as crescentic glomerulonephritis, PECs proliferate [4]. In addition, PECs are adjoined by tight junctions and together with the Bowman's basement membrane (BBM), serve as a second glomerular barrier to filtered protein [5].

The glomerular filtration barrier consists of the fenestrated endothelial cells, the glomerular basement membrane and podocytes [6]. Micropuncture studies in normal rats indicate that even in health, some albumin crosses the glomerular filtration barrier into the urinary space [7]. Others would even say that massive amounts are normally filtered [8]. PECs are positioned between the main glomerular filtration barrier and the proximal tubule and are therefore in a prime position to potentially act as a sensor for kidney health. Moreover, we reported that injury to PECs in disease leads to 'leakiness' of filtered tracers beyond the glomerulus [5]. The purpose of this study was to define the interaction of PECs and filtered albumin and to determine if albumin was injurious to these cells.

Materials and methods

Animal models

To determine if albumin internalization increased in PECs during proteinuric diseases, four well characterized models of experimental glomerular disease characterized by proteinuria were used for study as follows:

Experimental protein overload models. Mouse model of protein overload nephropathy: Experimental protein overload nephropathy induced by bovine serum albumin (BSA) is a non-immunological model of proteinuria and tubulointerstitial fibrosis. To induce the albumin overload model in mice, four female Balb/c mice weighing ~20 g (7 weeks of age) were fed a standard diet with free access to water. Mice were given daily intraperitoneal (IP) injections of BSA (Sigma A-9430; Sigma) dissolved in saline (200 mg/mL) for 8 days as follows: Day 1 = 2 mg BSA/g body weight, Days 2–5 = daily doses increasing by 2 mg BSA/g body weight to a final dose of 10 mg BSA/g body weight on Day 5. No injections were given on Days 6 and 7 and a final dose of 10 mg BSA/g body weight was given again on Day 8. This dosing regimen is similar to what we have previously reported [9]. Mice were weighed daily prior to BSA administration. Control mice received no BSA ($N = 3$ per group). Mice were placed into individual metabolic cages overnight and spontaneously voided urine was collected for 12 h prior to BSA administration, Days 3–4 following BSA administration and prior to sacrifice for determination of urinary protein to creatinine ratios. Urine protein was determined using the sulfosalicylic method [10] and urine creatinine was determined using a colorimetric microplate assay (Oxford Biomedical Research, Oxford, MI and Cayman Chemical Company, Ann Arbor, MI), as we have previously reported [11]. Animals were sacrificed by cervical dislocation and kidney tissue was harvested and processed for additional studies.

Rat model of protein overload nephropathy. This model was induced as previously reported [12] in female Sprague–Dawley rats weighing 90–110 g. A right nephrectomy was performed on each animal 5–7 days before the initiation of IP injections. Animals were given 1.0 g BSA (Sigma A-7906; Sigma) per 100 g body weight dissolved in saline daily for 3 weeks. Control animals received an equivalent volume of saline ($N = 6$ per group).

Puromycin aminonucleoside nephropathy model of experimental minimal change nephropathy. Puromycin aminonucleoside (PAN) nephropathy was induced in male Sprague–Dawley rats aged 60 days (200–300 g) by injecting a single dose of puromycin aminonucleoside dissolved in 0.9% NaCl at 6 mg/100 g body weight via tail vein as previously reported [11]. Control animals were injected with an equal volume 0.9% NaCl ($N = 6$ per group). At Day 7 following injection, animals were sacrificed and tissues were obtained for renal biopsies.

Passive Heymann nephritis model of experimental membranous nephropathy. Passive Heymann nephritis (PHN) nephropathy was induced in male Sprague–Dawley rats (200–250 g) by IP injection (5 mL/kg) of sheep antibody to Fx1A as previously reported [13]. A control group of rats received equivalent volumes of normal sheep serum. Control and PHN animals were sacrificed on Days 5, 10 and 30 following disease induction ($N = 6$ per group at each time point).

Adriamycin nephropathy model of experimental focal segmental glomerulosclerosis. Adriamycin (ADR) nephropathy was induced in male Balb/c mice, aged 12 weeks by tail vein injection of ADR 12 mg/kg body weight × 2 separated by a 4-week period, as previously reported [14]. Control animals were injected with an equal amount of vehicle only (0.9% NaCl). ($N = 3$ per group). At Day 14 following injections, animals were sacrificed and tissues were obtained for renal biopsies.

The University of Washington Animal Care Committee approved all experimental protocols. All animal procedures were conducted in accordance with the Institutional Animal Care and Use Committee.

Cell culture

A conditionally immortalized mouse parietal epithelial cell line (mPEC RYFP 4a) was generated as previously described [15]. In brief, H-2Kb-tsA58 mice, also called Immortomice (The Jackson Laboratory, Bar Harbor, ME), containing an interferon (IFN)-γ inducible promoter for expression of thermo-sensitive SV40 large T antigen were intercrossed with KSPcre × Rosa26YFP mice (gift of Fangming Lin, University of Texas Southwestern), which express yellow fluorescent protein in PECs. PECs were isolated from Bowman's capsule-containing glomerular outgrowths by fluorescent cell sorting and were characterized by immunostaining and western blotting to cell-specific proteins as previously described [15, 16]. Cells were initially cultured in growth permissive conditions on Primaria plastic plates (BD Biosciences, Bedford, MA) coated with collagen I (BD Biosciences) at 33°C with IFNγ (5 μL/10 mL media; BD Biosciences) in RPMI media (SH3025501; Fisher Scientific, Pittsburgh, PA) with 5% fetal bovine serum (FBS), penicillin/streptomycin (Sigma–Aldrich, St Louis, MO) and sodium pyruvate (Fisher Scientific). Cells were then differentiated in growth-restricted conditions for at least 12 days by switching them over to 37°C without IFNγ. Fully differentiated cells were incubated with fatty acid free, low endotoxin BSA (Sigma A8806) at increasing doses (40–40 000 μg/mL) for 0, 6, 24 and 48 h in RPMI media with 5% FBS. These doses include physiologic concentrations to nephrotic levels, which is similar to that used in apoptosis studies of proximal tubular cells [17]. The BSA concentration in media was pH adjusted with Bioreactor pH Adjustment Solution, 200 μL/10 mL BSA concentration (Sigma B 1185; Sigma). mPECs used were between passages 12 and 25. HEK293 cells (ATCC) were cultured under standard conditions at 37°C in Dulbecco's modified Eagle's media (Invitrogen, Carlsbad, CA).

Immunohistochemistry

Indirect immunoperoxidase staining was performed on kidney biopsies from mice and rats on neutralized formalin-fixed, paraffin-embedded sections as previously reported [16]. In brief, de-paraffinization was performed with Histoclear (National Diagnostics, Atlanta, GA) and sections were rehydrated in graded ethanol. Antigen retrieval was performed by microwaving sections in 10 mM citric acid buffer, pH 7.0 [BSA and phosphorylated extracellular signal-regulated kinase 1 and 2 (p-ERK1/2)], 10 mM citric acid buffer, pH 6.0 (albumin), 10 mM ethylenediaminetetraacetic acid (EDTA), pH 6.0 (PAX 8) and enzyme digestion with protease XIV for megalin and FcRn (Sigma). Endogenous peroxidase activity was quenched with 3% hydrogen peroxide and non-specific protein binding was blocked with Background Buster (Accurate Chemical & Scientific Corp., Westbury, NY). Endogenous biotin activity was quenched with the Avidin/Biotin blocking kit (Vector Laboratories, Burlingame, CA). After blocking, tissue sections were incubated overnight at 4°C with primary antibody. Slides were then washed with phosphate-buffered saline (PBS) and incubated with the appropriate biotinylated secondary antibodies: anti-rabbit IgG (Vector Laboratories), anti-chicken IgG (Vector Laboratories), anti-mouse IgG (Vector Laboratories) and anti-goat IgG (Jackson ImmunoResearch Laboratories, Inc, West Grove, PA) for 1 h followed by R.T.U. Vectastain kit (Vector Laboratories). Staining was visualized by precipitation of diaminobenzidine (DAB; Sigma). Nuclei were counterstained with hematoxylin and, in some cases, periodic acid Schiff staining was also performed. Omission of the primary antibody was used as a negative control. Antibodies used were chicken polyclonal anti-albumin 1:200 (PA1-25673; Thermo Scientific, Rockford, IL), rabbit polyclonal anti-BSA 1:10K (RAB/Alb/7S Nordic Immunology, The Netherlands), mouse monoclonal anti-megalin/gp330 1:400 (NB110-96417; Novus Biologicals, Littleton, CO), goat polyclonal anti-cubilin 1:50 (sc-20609; Santa Cruz Biotechnology, Santa Cruz, CA), goat polyclonal anti-FcRn 1:500 (sc-46328 Santa Cruz), rabbit polyclonal anti-phospho-p44/42 MAPK [extracellular signal-regulated kinase 1 and 2 (ERK1/2)] (Thr202/Tyr204) 1:1000 (9101L; Cell Signaling Technology, Boston, MA), p44/42 MAPK (ERK1/2) 1:1000 (9102; Cell Signaling Technology) and rabbit polyclonal PAX 8 1:500 (10336-1-AP Protein Tech Group, Inc, Chicago, IL).

Confocal microscopy

Immunofluorescence staining for native albumin and for BSA (in protein overload models) was performed on kidney biopsies from mice and rats on neutralized formalin-fixed paraffin-embedded sections. De-paraffinization and rehydration was performed as described above using the same antigen retrieval procedures for albumin and BSA, followed by Background Buster (Accurate Chemical & Scientific Corp.). The primary antibody was applied overnight, followed by incubation with Alexa488-conjugated anti-rabbit and anti-chicken secondary antibodies (Invitrogen, Carlsbad, CA) for 1 h. Hoechst 33342 was added to the secondary antibody incubation step for labeling of nuclei. Sections were mounted in Slow Fade Gold mounting media (Invitrogen) and coverslip applied. Confocal images were performed on a Zeiss 510 Meta microscope.

Fluorescence-activated cell sorting

Fluorescence-activated cell sorting (FACS) analysis was used on cultured cells to measure albumin internalization and the effects of endosomal inhibition on this process. Cultured PECs were grown in RPMI media with 2% FBS in growth-restricted conditions for a minimum of 12 days and changed to serum-free conditions for 16–24 h prior to FACS analysis. mPECs were exposed to 40 μg/mL fluorescein isothiocyanate (FITC)–BSA (Sigma) for 1 h in the presence or absence of 5-*N*-ethyl-*N*-isopropyl amiloride (EIPA; Sigma) 130 μM, an endosomal inhibitor, for 15 min prior to FITC–BSA [18, 19]. Control mPECs were not exposed to FITC–BSA. Cells were washed with Hank's-buffered salt solution (Invitrogen) five times, detached with trypsin (Irvine Scientific, Santa Ana, CA) and centrifuged at 2500 r.p.m. for 7 min. Cell pellet was re-suspended in 200 μL Trypan Blue 0.4% (Sigma) and transferred to polystyrene tubes (BD Falcon, Bedford, MA). Internalized FITC-labeled BSA fluorescence was measured by quenching external fluorescence using a method similar to that described by others [20, 21]. Since the light absorption range of trypan blue is 475–675 nm and covers the wavelength of fluorescein fluorescence emission (519 nm), the fluorescence of externally bound FITC–BSA is quenched by trypan blue and any fluorescence detected is from FITC–BSA that has been internalized by the mPECs. FACS analysis was performed on the BD LSRII Flow Cytometer (BD Biosciences, San Jose, CA) and analysis performed with FlowJo software version 9.1. Gating parameters for mPECs analyzed were defined for a subpopulation of mPECs and was standardized for all experimental groups. A minimum of 10 000 cells was measured in each sample. The results of three separate FACS experiments were analyzed.

Apoptosis detection

In vivo measurements. Terminal deoxynucleotidyl transferase (TdT)-mediated deoxyuridine triphosphate nick end labeling (TUNEL) staining was performed based on a modified protocol as previously described [14] to determine whether apoptosis occurred following exposure to BSA. TUNEL staining was performed on 4-μm formalin-fixed paraffin-embedded kidney tissue sections from mice and rats. De-paraffinization and rehydration was performed as described above. Antigen retrieval was performed by boiling sections in 10 mM citric acid buffer pH 7.0. Nuclei were permeabilized by incubation with proteinase K (Roche Diagnostics, Indianapolis, IN) for 20 min at room temperature. Following incubation in TdT buffer (Invitrogen) for 5 min, fragmented DNA was labeled by exposure to biotin-14-deoxyadenosine triphosphate (dATP) (Invitrogen) in TdT buffer for 60 min at room temperature. The reaction was terminated by washing in PBS followed by blocking in 2% BSA in water for 10 min at room temperature. Development was performed by incubating section with R.T.U. Vectastain kit for 30 min at room temperature for signal amplification followed by DAB (Sigma) with $NiCl_2$ as chromagen. Slides were counterstained in hematoxylin, dehydrated and coverslipped.

In vitro measurements. mPEC apoptosis was measured by staining with 10 mM Hoechst 33342 in non-fixed cells. Apoptosis was defined by the presence of chromatin condensation and formation of apoptotic bodies. A minimum of 300 cells per well was counted per experimental condition using inverted fluorescent microscopy. All experiments were performed a minimum of three times [14, 22–24].

Measuring cell number. A non-radioactive [3-(4,5) dimethylthiazol-2,5-diphenyltetrazolium bromide] (MTT) assay (Promega, Madison, WI) was performed according to the manufacturer's instructions to identify living cells based on the cellular conversion of a tetrazolium salt into a formazan product, which was quantified by spectrophotometry. Briefly, cultured mPECs were plated into 24-well plates in growth-restricted conditions for 12–16 days. BSA (40 000 μg/mL) was added to half of the wells for 6, 24 and 48 h. BSA was removed, cells were washed in PBS and standard media (PRMI 1640 media with 5% FBS) was added back to the wells. A labeling dye from the kit was added for 1–4 h at 37°C followed by addition of stop solution to terminate the reaction and solubilize the cells for at least 1 h. A reference absorbance was read at 650 nm and subtracted from the absorbance read at 570 nm. A minimum of 10 wells was read at each time point. Experiments were performed in quadruplicate [25].

Subcellular protein fractionization

Isolation of membrane and cytosolic protein fractions of growth-restricted mPECs exposed to BSA was performed to distinguish between BSA uptake into the cell from simple binding of BSA to the cell membranes using a modified procedure as previously reported [24]. Cells were lysed and suspended in CLB buffer (10 mM Tris pH 7.5, 300 mM sucrose, 1 mM EDTA) (Sigma–Aldrich) containing protease inhibitors (Roche Molecular Biochemicals, Indianapolis, IN), 1 mM Na-orthovanadate (Sigma), 50 mM NaF (Sigma) and 1 mM phenylmethlysulfonyl fluoride (Sigma). After incubation on ice for 10 min with vigorous vortexing, lysates were centrifuged at 4°C at 780 *g* for 2 min. Supernatant was transferred to a separate tube and centrifuged at 4°C at 12 500 *g* for 20 min. Supernatant from this step was transferred to a Beckman centrifuge tube and spun at 4°C at 100 000 *g* for 60 min resulting in a membranous enriched fraction (pellet) and cytosolic protein fraction (supernatant). The pellet was washed with CLB and spun again with supernatant from previous step at 100 000 g for 60 min. The pellet was resuspended in TSE buffer (10 mM HEPES, 10 mM NaCl, 1 mM KH_2P0_4, 5 mM $NaHC0_3$, 1 mM $CaCl_2$, 0.5 mM $MgCl_2$) in total 300 mM NaCl. Protein concentration was determined by BCA protein assay kit (Pierce Biotechnology, Rockford, IL), and western blot analysis was performed using anti-BSA antibody. Cultured mPECs not exposed to excess BSA served as controls.

Western blot analysis

Protein levels for BSA, total ERK1/2, p-ERK1/2, megalin, cubilin and FcRn were measured by western blot analysis as previously reported [11]. Protein samples were lysed and suspended in RIPA buffer (50 mM Tris–HCl, pH 8.0, 5 mM EDTA, 150 mM NaCl, 1% Triton X-100, 1% NP-40) containing a protease inhibitor cocktail (Roche Diagnostics) with 1 mM sodium orthovanadate. Lysates were cleared by centrifugation and protein concentration determined by BCA protein assay kit (Pierce Biotechnology) according to the manufacturer's protocol. Reduced protein samples (10–20 μg) (BSA, total ERK1/2 and p-ERK1/2) and non-reduced protein samples (megalin, cubilin, and FcRn) were separated on sodium dodecyl sulfate (SDS)–polyacrylamide electrophoresis gels and subsequently transferred to polyvinylidine difluoride membranes (Hybond-P). After blocking with 5% non-fat dry milk in Tris-buffered saline (10 mM Tris–HCl, pH 8.0, 150 mM NaCl) containing 0.1% Tween 20, membranes were incubated overnight at 4°C with primary antibody. Membranes were washed with Tris-buffered saline-T and incubated with an appropriate biotinylated secondary antibody. Protein bands were visualized with ECL plus (GE healthcare Bio-Sciences, Piscataway, NJ) and developed with a gel imaging system (Bio-rad Chemidoc). Membranes were then stripped (100 mM glycine, 1% SDS, pH 2.5) and western blot analysis was repeated for loading control proteins. Band densitometry was performed using ImageJ (Rasband, W.S., ImageJ, U. S. National Institutes of Health, Bethesda, Marylandhttp://rsb.info.nih.gov/ij/, 1997–2009.) and background was subtracted from each blot.

Plasmid transfection of constitutively active mitogen-activated protein kinase 1

p-ERK1/2 levels were increased by retroviral infection with constitutively active mitogen-activated protein kinase (MEK) 1 similar to previously described methods [26]. In brief, pBabe vectors encoding MEK-DD (Addgene plasmid 15268) and empty vector were transfected into Phoenix Eco packaging cells to generate retrovirus [27]. The retrovirus-containing media were harvested and filtered onto sub-confluent, proliferating mPECs in growth permissive conditions. Selection of infected cells was performed by 48 h selection with puromycin 1.0 μg/mL (Sigma–Aldrich) and passaged into growth-restricted conditions. Western blot analysis confirmed overexpression of p-ERK1/2 in transfected mPECs. Cells were exposed to BSA 40 000 μg/mL and apoptosis was measured by Hoechst 33342 counting as detailed above.

Inhibition of ERK phosphorylation

Inhibition of p-ERK1/2 was performed using the MEK 1/2 inhibitor U0126 (Cell Signaling Technology) according to the manufacturer's protocol. Briefly, cultured mPECs in standard medium were incubated with U0126 (10 μM) or dimethyl sulfoxide (DMSO) (vehicle) for 1 h prior to the addition of excess BSA for 6, 24 and 48 h. The cells were exposed to U0126 every 12 h due to its short half-life. The percentages of apoptotic cells were measured by Hoechst staining as described elsewhere in this section. Western blot analysis was performed to confirm MEK 1/2 inhibition.

Statistical analysis

Statistical analysis was performed using GraphPad Prism version 5.02 for Macintosh (GraphPad Software, San Diego, CA); statistical significance was evaluated using unpaired *t*-test. Results are reported as mean ± SEM. A P-value of <0.05 was considered to be statistically significant.

Results

PECs internalize albumin under normal conditions

Given that PECs are positioned between the main glomerular filtration barrier and the proximal tubular cells, we examined the potential role of PECs in taking up albumin under normal conditions. Immunoflourescent staining for native albumin was performed in non-diseased normal mice and rats, and multiple images were taken through the thickness of the section by confocal microscopy. As expected, albumin staining was observed in the capillary loops of the glomerulus. Albumin staining was also visualized inside the PECs as seen on Z-series images, confirming internalization of albumin by PECs. Representative images are shown in Figure 1 (A and B magnified inset). No staining was observed in the negative control (C). Native albumin staining intensity was light to moderate and was cytoplasmic. Glomeruli exhibited a heterogeneous staining pattern, in that some glomeruli had very little or no PECs stained for albumin, whereas other glomeruli had part of their PECs stained for albumin and some had all PECs stained around the entire circumference of the glomerular cross section.

In order to quantify the amount of albumin internalized by PECs, staining for native albumin by immunohistochemistry (IHC) was scored. In order to more accurately demonstrate the distribution of the staining described above, the scoring system was based on the percentage of PECs staining positive (0, 25, 50, 75 and 100%). Mice typically have a fraction of their glomerular circumference occupied by the proximal tubule; however, this is typically not present in rats. Since the proximal tubule cells may not be easily discerned from PECs, a portion of the albumin score might also be attributed to the tubular uptake of albumin. However, albumin internalization was observed in PECs in normal conditions. Figure 1D shows the distribution of scores for each individual glomerulus in non-diseased mice. As demonstrated by the distribution, some glomeruli had no PECs staining, some had 100% of the PECs staining, but most fell somewhere in between. The mean of these scores was 49.04 ± 1.96. Similarly, Figure 1E shows the distribution of scores for each individual glomerulus in control

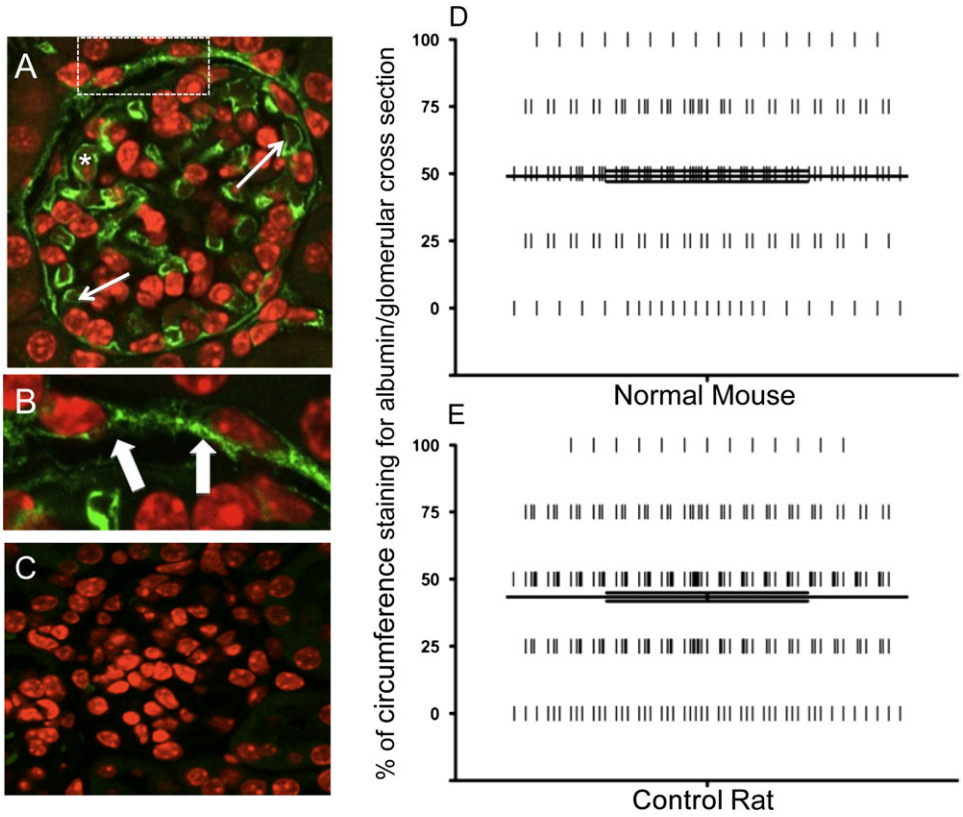

Fig. 1. Native albumin is internalized by PECs under non-diseased conditions. (**A**–**C**) Representative confocal microscopy images of immunofluorescent staining for native albumin (green) and nuclei (red) in non-diseased balb/c mice. (**A**) Albumin staining was detected in PECs (inset), podocytes (asterisk) and glomerular endothelial cells (thin arrows). (**B**) Shows a higher magnification of the inset of PEC staining shown in Panel A. The wide arrows represent cytoplasmic albumin staining in PECs. (**C**) No albumin staining was detected when the primary antibody is omitted. Quantification of albumin staining was performed (**D** and **E**). Individual glomeruli were scored based on the percentage of the glomerular circumference staining for albumin. (D) Hash marks represent the score for each glomerulus in non-diseased mouse and (E) control rats. The mean of the scores is represented by the horizontal line with error bars indicating the SEM.

rats. The mean of the scores in control rats was 43.34 ± 1.56. Representative images of native albumin staining for each score are shown in Figure 2A–E mice and in Figure 2F–J rats.

These results show that PECs take up albumin under normal conditions in mice and rats. Additionally, PECs in individual glomeruli internalized albumin to widely varying degrees. As expected, staining was not detected when the albumin primary antibody was omitted (data not shown).

Albumin internalization is increased in PECs in experimental proteinuric models. To test the hypothesis that albumin internalization is further increased when PECs are exposed to increased amounts of filtered albumin, several animal models of glomerular diseases characterized by increased albuminuria were studied. Quantification was performed by IHC and each individual glomerulus was given an albumin staining score as described above. Firstly, the PAN-induced nephrosis model of minimal change disease was studied at Day 7. Figure 3A shows the rat albumin staining score distribution for each individual glomerulus in PAN controls (left column) and PAN Day 7 (right column). There was a statistically significant increase in the mean of the scores (58.80 ± 1.63 PAN versus 26.10 ± 1.34 Control, $P < 0.0001$).

Secondly, the ADR mouse model of focal segmental glomerulosclerosis (FSGS) was examined. Figure 3B shows the mouse albumin staining score distribution for each glomerulus in ADR controls (left column) and ADR Day 14 (right column). Again, there was a statistically significant increase in the mean score in ADR versus ADR controls (62.67 ± 1.82 ADR versus 46.81 ± 2.12, $P < 0.0001$).

Thirdly, the score distribution of staining for rat albumin in each individual glomerulus in the PHN model of membranous nephropathy are shown in Figure 3C–E, PHN controls (left columns) and PHN disease (right columns). There was a statistically significant increase in the mean score at Day 5 (40.51 ± 3.64 PHN versus 30.00 ± 3.52 Control, $P = 0.04$), Day 10 (59.57 ± 2.33 PHN versus 32.37 ± 2.36 Control, $P < 0.0001$) and Day 30 (58.49 ± 2.81 PHN versus 35.40 ± 2.19 Control, $P < 0.0001$). Note that in all of the models examined, there was a similar shift. Less glomeruli with no staining were observed in disease and more glomeruli with scores of 50, 75 and 100% were observed. This indicates that in states of increased albumin, more PECs take up albumin. All these models were characterized by an increase in native albumin; we next examined a model of increased albumin from an exogenous source.

Experimental protein overload models were induced in mice and rats by IP injections of BSA. There was no statistically significant difference in albuminuria in control mice not given BSA and the albuminuria at Day 0 in the protein

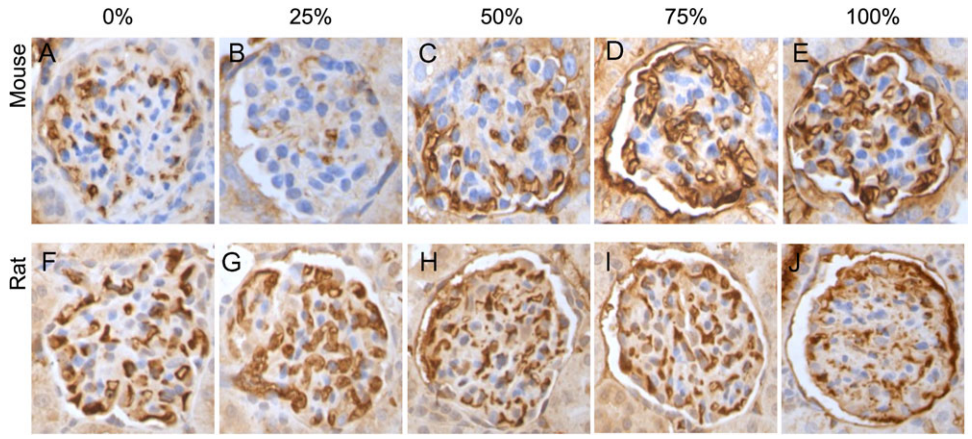

Fig. 2. Native albumin staining in experimental proteinuric overload models. Representative images of IHC for native albumin in mouse (**A**–**E**) and rat (**F**–**J**). Individual glomeruli were scored based on the percentage of the glomerular circumference staining for native albumin in each glomerular section. (A and **F**) represent absence of PEC staining (0%) in mouse and rat, respectively. (B and G) represent PEC staining around ~25% of the glomerular circumference. (C and H) represent PEC staining around ~50% of the glomerular circumference. (D and I) represent PEC staining around ~75% of the glomerular circumference. (E and J) represent PEC staining around ~100% of the glomerular circumference.

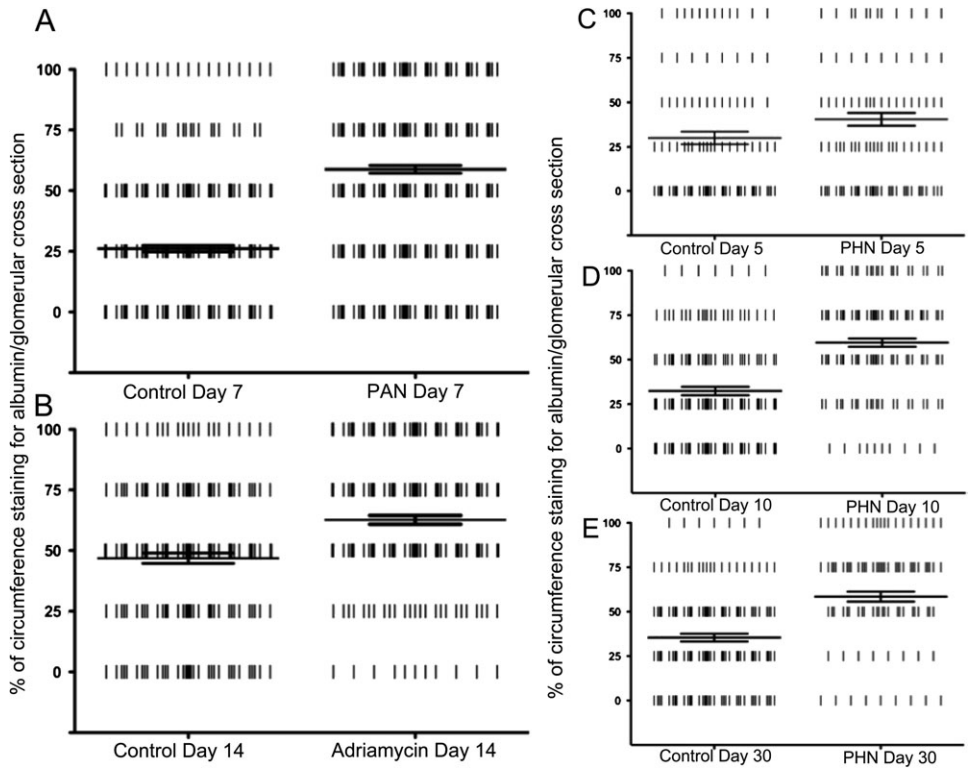

Fig. 3. Scatterplot representing albumin staining score in proteinuric disease models. (**A**) There was a statistically significant increase in the mean of the scores for albumin staining the circumference of the glomerulus at Day 7 in PAN rats (right column) compared to controls (left column). (**B**) There was a statistically significant increase in the mean of the scores at Day 14 in ADR mice (right column) compared to Day 14 controls (left column). (**C**) PHN Day 5, (**D**) PHN Day 10 and (**E**) PHN Day 30 rats all had statistically significant increases in the mean of the scores (right columns) compared to their same day controls (left columns).

overload mice (12.5 ± 0.75 mg/dL versus 46.13 ± 18.59 mg/dL, $P > 0.05$). On Day 9 of protein overload nephropathy in mice, there was a statistically significant increase in albuminuria compared to Day 0 (168.5 ± 39.27 mg/dL versus 46.13 ± 18.59 mg/dL, $P = 0.03$). Representative confocal images of FITC–BSA in the mouse are shown in Figure 4.A, with a higher magnification image in Figure 4B. IHC for BSA was performed and staining in PECs was quantitated in the same manner described above. The results for the BSA staining score distribution in the protein overload models are shown in Figure 4C and D (right columns) and compared with control animals that did not receive BSA (left columns). The BSA staining intensity was similar to proximal tubular cells, used as an internal positive control. We also confirmed BSA staining in podocytes as previously reported [28], another internal control. There was a significant increase in

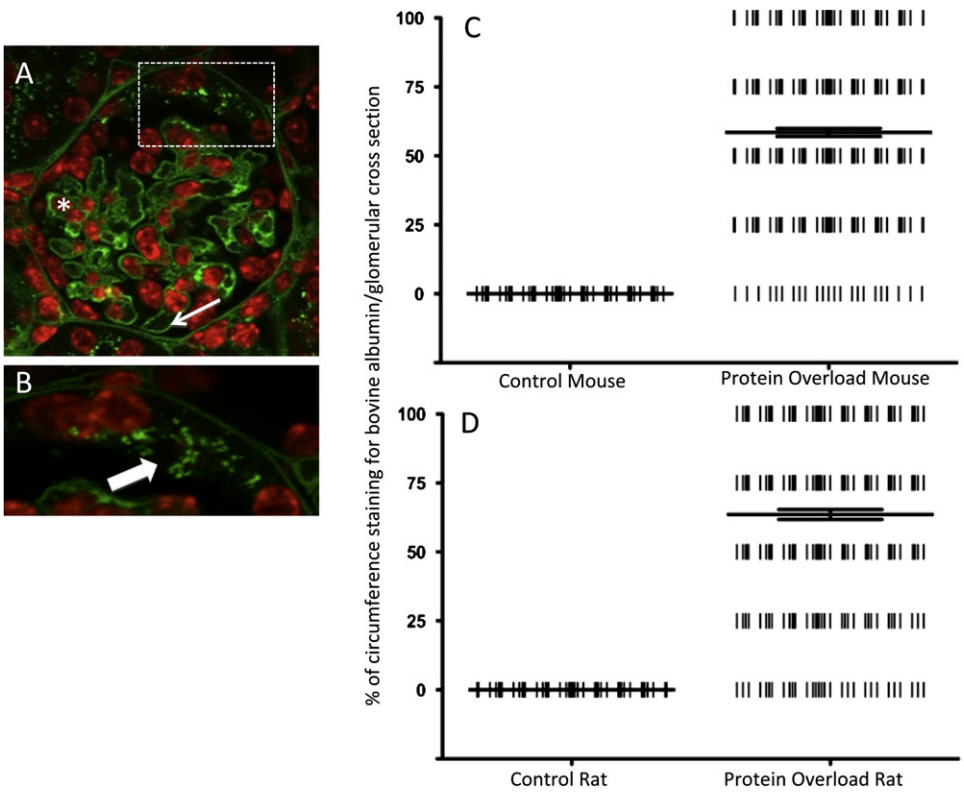

Fig. 4. BSA is internalized in PECs in experimental protein overload models in mouse and rat. (**A** and **B**) Representative confocal microsopy images of FITC-labeled BSA (green) and nuclei (red) in the mouse experimental protein overload model. (**A**) FITC–BSA is detected in PECs (inset), podocytes (asterisk) and glomerular endothelial cells (thin arrow). (**B**) A higher magnification of the inset shown in Panel A. The wide arrow indicates cytoplasmic FITC-labeled BSA in PECs. (**C**) Mouse and (**D**) Rat individual glomeruli were scored based on the percentage of the glomerular circumference staining for BSA in experimental protein overload nephropathy (right columns) compared to control animals that did not receive BSA (left columns). Hash marks represent the score for each glomerulus. The mean of the scores is represented by the horizontal line with error bars indicating the SEM.

the mean score in both mouse shown in Figure 4C (58.49 ± 1.45 versus 0) and rat shown in Figure 4D (63.57 ± 1.78 versus 0) protein overload models compared to control animals. As expected, no BSA was detected in mice and rat controls that did not receive BSA. In addition, no staining was present when the BSA primary antibody was omitted (figure not shown). These data show that there was marked internalization of filtered albumin by PECs and that the number of glomeruli involved and the number of PECs in each glomerulus internalizing albumin increased in several models of glomerular diseases characterized by increased albumin filtration.

Cultured mPECs internalize albumin

Next, cultured mPECs were used to validate the results of albumin internalization *in vivo*. Western blot analysis was performed on protein lysates from cultured mPECs exposed to BSA and the results are shown in Figure 5A. PEC whole cell lysates exposed to 40 000 μg/mL BSA showed increased BSA levels compared to control mPECs exposed to media alone. Since a small amount of BSA is present in the FBS used to supplement the media, the faint band for BSA was expected in control mPECs not exposed to excess BSA (40 000 μg/mL).

In order to show that the data were not simply due to non-specific binding of BSA to the membrane surface of the PECs, subcellular protein fractions were used to obtain membrane and cytosolic-enriched fractions (Figure 5A). Western blot analysis showed increased BSA in the cytosolic fraction of BSA-exposed mPECs compared to media alone. While overall less than the cytosolic fractions, there was a slight increase in BSA detected in the membrane fractions of mPECs exposed to excess BSA compared to mPECs exposed to media alone. Ponceau S staining of this membrane is shown in lieu of western blot analysis for a loading control protein as the membrane loading control, sodium potassium pump enzyme (Na/K ATPase) required non-reduced conditions and the anti-BSA antibody required reduced conditions, so both could not be detected on the same blot. The protein samples for whole cell lysate, membrane fraction and cytosolic fractions were evenly loaded. These data are consistent with albumin internalization in PECs.

To validate the western blot results above, FACS analysis was performed on cultured mPECs exposed to FITC–BSA (40 μg/mL) in the presence and absence of an endosomal inhibitor. Representative histograms are shown in Figure 5B–D. The results of three separate experiments were combined and the median fluorescence intensity (MFI) of mPECs exposed to FITC–BSA are shown in Figure 5E, Column 2 (209 ± 7.1) As expected, this was significantly higher than the MFI of mPECs not exposed to FITC–BSA (Figure 5E, Column 1, 97 ± 4.9, $P < 0.0002$).

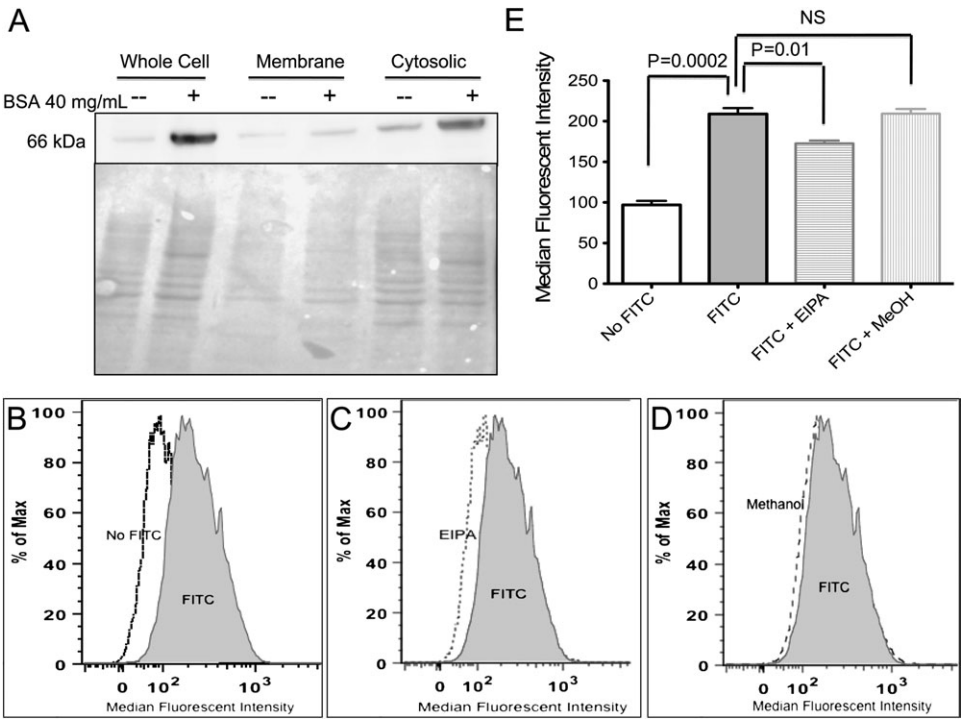

Fig. 5. Albumin internalization in cultured mPECs. (**A**) Western blot analysis for BSA in cultured mPECs exposed to 40 000 μg/mL BSA. More BSA was detected in whole cell lysate from PECs exposed to excess BSA (Lane 2) compared to control cells (Lane 1). More BSA was also detected in the cytosolic fraction from PECs exposed to BSA (Lane 6) compared to PECs that were not exposed to excess BSA (Lane 5), indicating internalization of BSA. Faint bands for BSA were detected in the membrane fractions in both PECs exposed to BSA (Lane 4) and PECs not exposed to BSA (Lane 3). (**B**–**D**) Representative histograms of FACS analysis performed on cultured mPECs exposed to FITC–BSA. The *x*-axis represents MFI and the *y*-axis is percentage of cells in the population measured. (B) Cultured mPECs not exposed to FITC–BSA (open area with dotted lines) have low MFI compared to mPECs exposed to FITC–BSA (shaded area with solid line), which had a significantly higher MFI. (C) In the presence of EIPA, an endosomal inhibitor, mPECs exposed to FITC–BSA (open area with dashed line) had a significantly decreased MFI compared to mPECs exposed to FITC–BSA (shaded area with solid line) without EIPA. (D) Control in which mPECs were exposed to FITC–BSA in the presence of methanol (open area with long dashes), the vehicle for EIPA, showed no significant decrease in MFI compared to mPECs exposed to FITC–BSA alone (shaded area with solid line). (**E**) Graphical representation of the average MFI from three separate FACS experiments. EIPA significantly reduced the MFI (Column 3) compared with mPECs not exposed to EIPA (Column 2) or the vehicle for EIPA, methanol (Column 4).

Albumin internalization is partially endosomally mediated

To investigate the possible role of endocytosis in the internalization of albumin in mPECs, an endosomal inhibitor, EIPA was incubated with mPECs prior to and during FITC–BSA exposure to determine if this would result in reduced uptake of FITC–BSA [28]. EIPA specifically inhibits the activity of Na^+-H^+ exchanger isoform 3 (NHE3), which then limits endosomal acidification and subsequently has been shown to reduce albumin endocytosis in cultured proximal tubular cells [19]. The MFI of mPECs exposed to FITC–BSA (40 μg/mL) in the presence of EIPA decreased to 172.7 ± 3.5, P = 0.01 (Figure 5E, Column 3). To ensure that the reduction in MFI was due to EIPA, FACS analysis was also performed in mPECs exposed to FITC–BSA in the presence of methanol, the vehicle for EIPA and the MFI was 209.3 ± 5.8 versus no methanol, P = NS (Figure 5E, Column 4). Taken together, these data provide further evidence for albumin internalization in mPECs and that this was at least in part mediated by endosomes.

Albumin-binding receptors are present on PECs

Megalin (gp330) and cubilin are two albumin-binding receptors in the proximal tubule [6, 29–31], and megalin is also expressed in podocytes *in vivo* and *in vitro* [32–34]. Since albumin uptake by PECs occurs by an endosomal-mediated process, the expression of these known albumin receptors was examined in PECs.

Megalin staining was detected in 9.64 ± 0.54 PECs/glomerulus in normal rat kidney, although the staining intensity was significantly less than the staining in the proximal tubule brush border. Staining also confirmed the presence of megalin in podocytes of non-disease rats, which was also fainter than tubular staining. Compared to rat PECs, mPECs only rarely exhibited staining for megalin, while staining for megalin/gp330 was present in the proximal tubule of mouse tissue (data not shown). One hundred and fifty glomeruli were evaluated per biopsy and only one PEC had positive staining for megalin/gp330. It was not surprising that megalin/gp330 staining was only rarely present in the glomerulus since mice are resistant to the antibody targeting gp330 in the PHN model of disease.

Cubilin is a co-receptor for megalin and staining was also performed for cubilin. Staining was detected for cubilin in 8.90 ± 1.11 PECs/glomerulus in normal rat kidney in a similar distribution and quantity as megalin. Megalin and cubilin expression was evaluated in cultured mPECs by western blot analysis and no bands were detected in protein lysates from cultured mPECs; however, both were present

in protein lysates from mouse kidney cortex, which served as a positive control. Additionally, expression of megalin was confirmed in protein lysates from cultured podocytes, but cubilin expression was absent, as has been shown by others [34, 35] (data not shown).

The neonatal Fc receptor for IgG (FcRn) has also been shown to bind albumin [36, 37]. Immunostaining for FcRn was positive in 0.056 ± 0.02 PECs/glomerulus in mouse and 0.19 ± 0.045 PECs/glomerulus in rat. Negative control in which the primary antibodies were omitted did not have positive staining**.** FcRn expression was examined by western blot analysis in cultured mPECs but experimental conditions could not be optimized with the antibody.

The expression of these albumin-binding receptors was examined in BSA overload conditions and the results were quantified**.** In the rat BSA overload model, megalin expression did not increase significantly at 3 weeks (10.75 ± 0.62 versus saline control, $P > 0.05$). Similarly, cubilin expression did not increase significantly at 3 weeks (9.60 ± 1.19 versus saline control, $P > 0.05$). FcRn also did not show a statistically significant increase in staining in the mouse or rat protein overload models (0.06 ± 0.01 and 0.14 ± 0.10, $P > 0.05$, respectively). This suggests that albumin uptake capacity of PECs via these receptors is likely not increased during protein overload states. Additionally, the expression of megalin and cubilin was examined *in vitro* in experimental BSA overload and *de novo* expression of these receptors was not detected.

BSA uptake by PECs leads to apoptosis

One might ask, what were the consequences, if any, of increased albumin uptake by PECs? To determine if PEC apoptosis was increased, the TUNEL assay was performed in the mouse and rat protein overload models, and the images are shown in (Figure 6). In non-diseased mice, there were no TUNEL-positive PECs detected of 286 glomeruli counted (Figure 6A); in non-diseased rats, we counted only two TUNEL-positive PECs of 152 gloms. Noteworthy was that the number of TUNEL-positive PECs increased in disease in the mouse (7 TUNEL-positive PECs of 373 glomeruli counted) and in the rat protein overload model (30 TUNEL-positive PECs of 241 glomeruli counted) (Figure 6C and D, respectively). Positive control for TUNEL staining was performed on p35 (−/−) mouse in which a ureter was obstructed, which is known to have increased susceptibility to tubular epithelial and podocyte apoptosis [22] (Figure 6E). Negative control in which biotin-14-dATP was omitted is shown in Figure 6F.

To validate these findings, cultured mPECs were exposed to increasing concentrations of 40, 400, 4000, and 40 000 μg/mL BSA and this too resulted in apoptosis. Hoechst staining was performed to detect apoptosis in live unfixed cells following 6, 24 and 48 h exposure to BSA. Hoechst staining was quantified and is shown in Figure 7. There was no increase in apoptosis at the 6 h time point. At 24 h, a statistically significant increase in apoptotic cells was observed only at the highest dose of BSA 40 000 μg/mL (18.11% ± 1.0% versus 3.39% ± 1.36%, $P < 0.0001$). By 48 h, there was a statistically significant increase in apoptotic cells in mPECs exposed to BSA 4000 μg/mL (5 ± 0.25% versus 1.98 ± 0.34%, $P = 0.0011$) and 40 000 μg/mL (39.77 ± 3.55% versus 2.84 ± 0.64%, $P < 0.0001$).

To determine if there was a decrease in mPEC number following exposure to increasing doses of BSA, cell number was measured by the MTT assay. There was a statistically

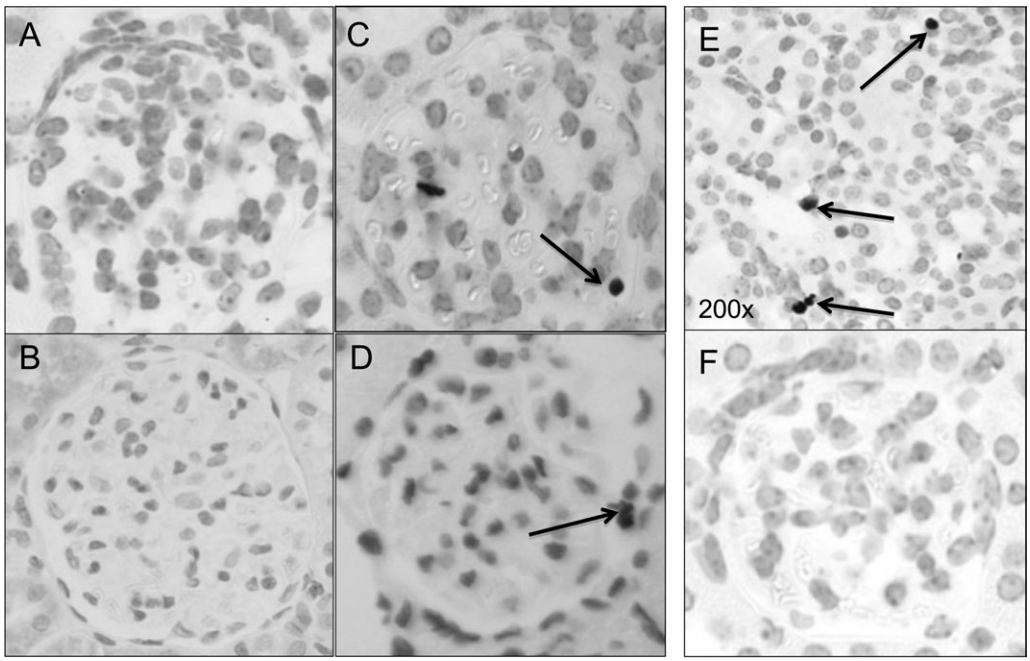

Fig. 6. Representative images of TUNEL staining for apoptosis detection. There were almost no positive TUNEL staining in PECs in non-diseased mice (**A**) and non-diseased rats (**B**). TUNEL staining in PECs was detected in BSA overload mouse (**C**) and rat (**D**). Staining was also detected in the positive control mouse tissue with unilateral ureteral obstruction (**E**). No staining was detected with omission of biotin-14-dATP labeling (**F**).

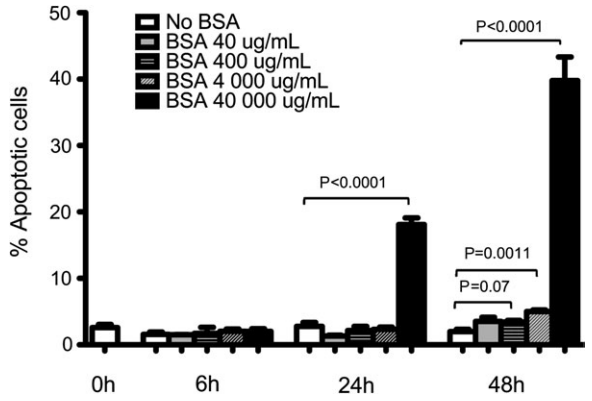

Fig. 7. Quantification of Hoechst-positive apoptotic cultured PECs exposed to increaing concentrations of albumin. Apoptosis increased significantly at 24 h (Column 11, solid black) and 48 h (Column 16, solid black) in mPECs exposed to 40 000 μg/mL BSA ($P < 0.0001$). Apoptosis also increased significantly at 48 h in mPECs exposed to a lower concentration, 4000 μg/mL BSA (Column 15, diagonal hashed, $P = 0.0011$).

significant decrease in relative absorbance (0.67 ± 0.06 BSA versus 1.04 ± 0.05 Control) at 48 h, $P < 0.0001$ (figure not shown) in mPECs exposed to 40 000 μg/mL BSA, indicating a decrease in cell number. Six replicates from each condition at each time point were analyzed and the experiments were performed in quadruplicate. Thus, exposure to excess albumin leads to BSA internalization, resulting in PEC apoptosis *in vitro*, leading to reduced cell number.

p-ERK1/2 is decreased in PECs exposed to BSA in vivo and in vitro

Having demonstrated BSA internalization and subsequent apoptosis occurs in PECs after excess albumin exposure, p-ERK1/2 levels, which in some cell types such as podocytes protects from apoptosis [38] were examined following BSA uptake in the protein overload model in mice. Figure 8A shows representative immunostaining for p-ERK1/2 in non-diseased mice and Figure 8B shows representative immunostaining in experimental protein overload mice. The staining results were quantified in Figure 8C and expressed as the percentage of p-ERK-positive PECs over total PECs per glomerular section as measured by PAX 8 staining described above. Interestingly, p-ERK1/2 was constitutively stained in normal PECs (Figure 8A). However, there was a statistically significant decrease in the percentage of PECs with p-ERK1/2 staining following BSA overload exposure in the mouse protein overload model (Figure 8C) (7.7 ± 0.88 versus 43.5 ± 2.79, $P < 0.0001$).

Western blot analysis for p-ERK1/2 in cultured PECs exposed to 40 000 μg/mL BSA was performed. Following BSA exposure, there was a quantitative decrease in protein levels for p-ERK1/2 in a time-dependent manner. Using ImageJ software, the background intensity was subtracted from the p44 and p42 band densities for each blot and the relative phosphorylated p44 and p42 to total ERK for each sample was calculated and normalized to 1 for unstimulated mPECs. The graph in Figure 8D shows a decrease in relative p-ERK1/2 levels by 2 h reaching less than half of the beginning levels by 6 h, which was sustained through 48 h.

Restoring p-ERK1/2 levels reduced apoptosis in PECs exposed to BSA

Since cultured mPECs exposed to 40 000 μg/mL BSA have reduced levels of p-ERK1/2 and increased apoptosis, we next sought to test the hypothesis that p-ERK1/2 protects PECs from apoptosis. Accordingly, cultured mPECs stably infected with MEK1, with resultant over-expression of p-ERK1/2 were exposed to 40 000 μg/mL BSA and compared to controls in which mPECs were stably infected with an empty vector and also exposed to 40 000 μg/mL BSA for 6, 24 and 48 h. Apoptosis was measured by Hoechst staining and the results are shown in Figure 9A. There was a statistically significant reduction in apoptosis in PECs over-expressing p-ERK1/2 compared to PECs infected with lentivirus carrying an empty vector when exposed to BSA. At 24 h, apoptosis was detected in $12.0 \pm 0.85\%$ PECs infected with empty vector versus $3.55 \pm 0.44\%$ in the PECs-over-expressing p-ERK1/2, $P < 0.0001$. At 48 h, $39.5 \pm 1.53\%$ of cells were apoptotic in the PECs infected with empty vector versus $19.76 \pm 5.52\%$ in the PECs over-expressing p-ERK1/2, $P = 0.0064$. Thus, normalizing p-ERK1/2 levels in PECs protected them from apoptosis when exposed to excess BSA. Western blot analysis was used to confirm over-expression of p-ERK1/2. There was indeed an increase in p-ERK1/2 following infection with MEK1 (Figure 9C, Lane 3) compared with no infection (Lane 1) and empty vector (Lane 2). Total ERK1/2 served as a loading control.

Inhibition of ERK1/2 phosphorylation increases apoptosis in PECs exposed to BSA. Finally, cultured mPECs were exposed to 40 000 μg/mL BSA for 6, 24 and 48 h in the presence of DMSO (vehicle) or U0126 (an inhibitor of ERK phosphorylation) and the results are shown in Figure 9B. Following inhibition of ERK phosphorylation, there was a statistically significant increase in apoptosis when PECs were exposed to BSA as measured by Hoechst stain compared to PECs exposed to BSA in the presence of DMSO. At 24 h, there was $11.42 \pm 0.54\%$ apoptosis in the DMSO group versus $32.31 \pm 0.46\%$ in the U0126 group, $P < 0.0001$. At 48 h, there was $56.42 \pm 5.48\%$ apoptosis in the DMSO group versus $78.62 \pm 0.65\%$ in the U0126 group, $P < 0.0158$. This data further suggest that the levels of p-ERK1/2 play a role in PEC survival following BSA uptake. Western blot analysis was used to confirm a decrease in p-ERK1/2. There was indeed a decrease in p-ERK1/2 in the presence of U0126 (Figure 9D, Lane 3) compared with mPECs exposed to media only (Lane 1) and DMSO, the vehicle for U0126 (Lane 2). Total ERK1/2 served as a loading control.

Discussion

The biological role(s) of PECs are not fully understood. They form a cell monolayer on BBM facing the urinary space with tight junctions between adjacent cells [1, 5]. Given their continued exposure to filtered albumin, the focus of the current research was to determine if there were consequences of increased albumin exposure and what they might be on PECs. We have recently shown that PECs, together with their tight

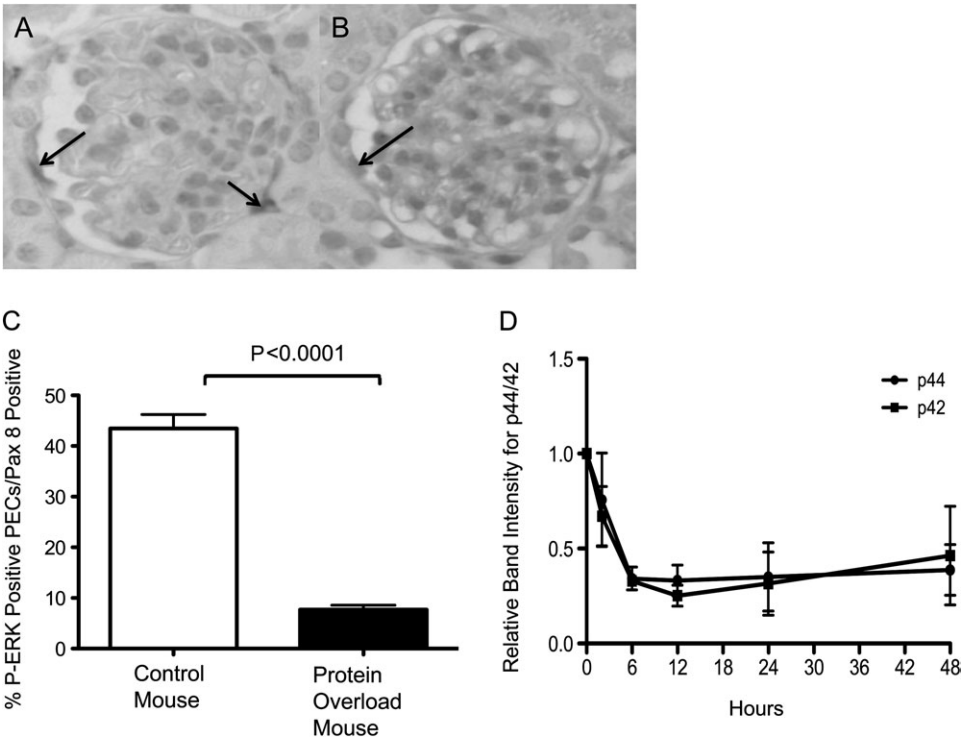

Fig. 8. IHC and western blot analysis for p-ERK1/2 *in vivo* and *in vitro*. Representative images of IHC for p-ERK1/2 in non-diseased mouse (**A**) and in mice with experimental protein overload model (**B**) No staining was detected in control staining in which primary antibody was omitted (not shown). (**C**) Quantification of p-ERK1/2 staining in PECs in non-diseased mouse (white column) and protein overload mouse (black column) shows a significant decrease in the percentage of p-ERK1/2-positive PECs in the mouse protein overload model compared to non-diseased mouse. Pax 8 staining was used to determine PEC number. (**D**) Graph of relative band intensities for p-ERK1/2 relative to total ERK 1/2 measured by western blot analysis of protein lysates from cultured PECs exposed to 40 000 μg/mL BSA. p-ERK1/2 decreases as early as 2 h and reached maximum from 6 h through 48 h.

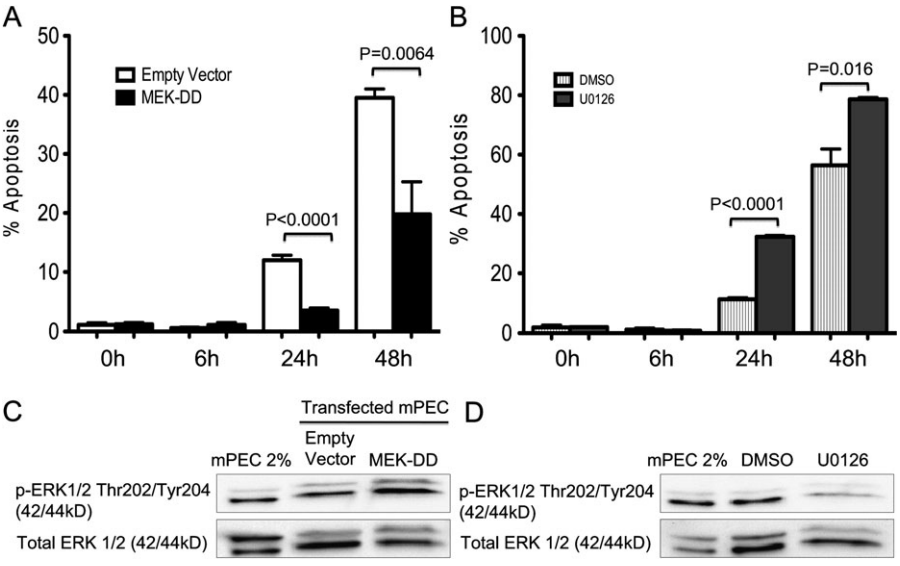

Fig. 9. (**A**) Quantification of apoptosis in cultured mPECs infected with MEK-DD, activator of MEK1 with resultant over-expression of p-ERK1/2 (black columns) exposed to BSA compared to mPECs infected with empty vector (white columns). There was a statistically significant decrease in apoptosis as measured by Hoechst staining in mPECs over-expressing p-ERK1/2 and exposed to BSA at 24 h (Column 6) and 48 h (Column 8) compared to mPECs infected with empty vector at 24 h (Column 5) and 48 h (Column 7). (**B**) Quantification of apoptosis in cultured mPECs exposed to BSA in the presence of DMSO, control vehicle (vertical striped columns) compared with U0126, an inhibitor of ERK 1/2 phosphorylation (gray columns). There was a statistically significant increase in apoptosis in mPECs exposed to BSA at 24 h (Column 6) and 48 h (Column 8) in the presence of U0126 compared to DMSO at 24 h (Column 5) and 48 h (Column 7). (**C**) Western blot analysis of p-ERK expression levels in mPEC (Lane 1), mPEC infected with empty vector (Lane 2) and mPEC infected with MEK-DD (Lane 3) confirms an increased p-ERK1/2 expression. (**D**) Western blot analysis of p-ERK1/2 expression levels in mPEC (Lane 1), mPEC treated with DMSO (Lane 2) and mPEC treated with U0126 (Lane 3) confirms reduced p-ERK1/2 expression following U0126. Total ERK expression served as loading controls.

junctions, function as a second glomerular barrier to limit protein from passing into the extraglomerular space [5]. We now show that a function of PECs is internalization of albumin and that when in excess, one consequence of this effect is apoptosis.

The first major finding in this study was that albumin is internalized by PECs of normal mice and rats as shown by both confocal microscopy and immunostaining. However, albumin internalization was markedly increased in several experimental glomerular disease models characterized by increased proteinuria due to podocyte injury. The PAN, ADR, PHN and protein overload models [39] are considered 'classic' podocyte diseases. In all four models, injury to podocytes leads to proteinuria. The BSA model has the added feature of excess albumin (BSA) delivery. Noteworthy was that PECs in all four models showed markedly increased staining for albumin.

A second finding of this study is that the pattern of albumin staining in PECs was heterogeneous. Our results showed that some glomerular sections only exhibited weak or absent albumin staining in PECs, while other glomeruli had substantially more intense staining around the entire glomerular circumference. Indeed, heterogeneous staining for albumin in tubules has also been described in a diabetic mouse model as well as proteinuric human diseases [40]. Those authors further analyzed serial sections and demonstrated that all glomeruli connected to albumin-positive tubules had albumin-stained lesions in the tuft that adhered to Bowman's capsule, implicating the relationship of albumin leakage to tubular damage. While the tubules and interstitial areas surrounding the glomeruli that had marked PEC staining for albumin in our proteinuric models were not noted to have significant injury as seen by our immunostaining methods, this is likely due to the early time points studied.

We used four methods to confirm albumin internalization in cultured PECs. Firstly, western blot analysis was used, showing that uptake was mainly confined to the cytosolic protein fraction. Secondly, FACS analysis of FITC–albumin internalization confirmed that albumin was not simply 'sticking' to the cell membrane. Thirdly, albumin internalization was reduced in the presence of an endosomal inhibitor. Fourthly, confocal microscopy confirmed albumin was 'inside' PECs. Taken together, the results show that PECs normally take up low amounts of filtered albumin and that the uptake increases markedly when PECs *in vivo* and *in vitro* are exposed to increased amounts of albumin. Thus, we can add PECs to the list of kidney cells taking up albumin.

We next attempted to address if a known albumin receptor was responsible for albumin internalization. A third finding in this study is that albumin-binding receptors are present normally on PECs. While albumin reabsorption in the proximal tubule has been well studied and the identification of albumin-binding receptors megalin and cubilin and FcRn [32, 33, 41, 42] have been reported, this is the first published report demonstrating that these receptors are also normally present in PECs. We demonstrated by immunostaining, the presence of megalin/gp330 and cubilin on rat PECs. While we also performed immunostaining in non-disease mouse kidneys as well as the BSA overload mouse model, we were not able to show convincing evidence for megalin/gp330 on mPECs. This is not surprising given that mice are resistant to the antibody-targeting gp330 in the Heymann Nephritis model. The neonatal receptor FcRn was also expressed by both mouse and rat PECs. While immunostaining for these three receptors was also performed in BSA overload models, there was no significant increase in the levels or number of cells expressing these receptors in disease. We recognize that these results may be false negatives due to the time frames studied. Additionally, the use of PECs in culture to study the role of megalin and cubilin in mediating albumin uptake is limited because megalin and cubilin are not expressed in mice. Further studies of the contributions of these receptors to albumin uptake and perhaps identification of other albumin-binding receptors would expand our knowledge in this area.

Having shown that a function of PECs in normal and albumin overload conditions is albumin internalization, we next asked what, if any, were the subsequent consequences. The fourth major finding was that increased albumin internalization is associated with apoptosis in PECs *in vivo* and *in vitro*. While the overall numbers of TUNEL-positive PECs were low in protein overload in mice and rats (~0.4% of PECs in mice and 0.9% in rats), this is likely due to the assay detecting only a small window of this apoptotic process. It is likely that we are underreporting the number of apoptotic PECs, as many more apoptotic cells have likely detached and likely washed away in the urinary ultrafiltrate. Indeed, PECs have been previously demonstrated in the urine of humans with proteinuric diseases [43]. We show that apoptosis also occurs in the cultured mPEC model and that this is accompanied by a reduction in cell number. Thus, as we have previously shown using tracer studies, PECs function as a second glomerular barrier to protein leakage into the extraglomerular space [5]. A proposed sequence of proteinuric disease progression is (i) PEC internalization of albumin (ii) PEC injury or loss and together with separation of tight junctions between PECs (iii) leakage of albumin through the BBM and (iv) subsequent interstitial inflammation and fibrosis.

Finally, we examined potential pathways whereby increased albumin internalization is associated with PEC apoptosis and focused on ERK signaling given its role in survival and death in different cell types. Of note is that PECs have a marked constitutive expression of p-ERK1/2. Albumin uptake *in vitro* and *in vivo* is associated with a marked decrease in p-ERK1/2 levels in PECs. A definite role of the ERK signaling pathway in BSA-induced apoptosis in cultured PECs was demonstrated. Forced overexpression of p-ERK1/2 was protective in BSA-induced apoptosis while reducing p-ERK1/2 levels substantially augmented albumin-induced PEC apoptosis. These data differ from work by Dixon and Brunskill who showed that recombinant human albumin stimulated proliferation of a cultured proximal tubular cell line at low levels (1 mg/mL) and that this is dependent on the ERK family of mitogen-activated protein kinases [44, 45]. Our data in PECs is similar to that of podocytes, where p-ERK1/2 is required for cell survival. Studies are ongoing to determine the biological consequences of PEC apoptosis.

In summary, we have shown that a functional role of PECs is albumin internalization, PEC uptake of albumin is heterogeneous and that PECs express known albumin-binding receptors. A consequence of prolonged exposure to high levels of albumin is PEC apoptosis, which is ameliorated by increasing ERK1/2 phosphorylation. Further studies into the biological roles of the PECs are ongoing.

Acknowledgements. We acknowledge the following investigators for providing research material used in this study: William C. Hahn (pBabe-puro-MEK-DD) and Fangming Lin (KSPcre x Rosa26YFP mice). This work was supported by NIH grant DK081835.

Conflict of interest statement. None declared.

References

1. Ohse T, Pippin JW, Chang AM *et al.* The enigmatic parietal epithelial cell is finally getting noticed: a review. *Kidney Int* 2009; 76: 1225–1238
2. Nadasdy T, Laszik Z, Blick KE *et al.* Proliferation activity of intrinsic cell populations in the normal human kidney. *J Am Soc Nephrol* 1994; 4: 2032–2039
3. Pabst R, Sterzel RB. Cell renewal of glomerular cell types in normal rats. An autoradiographic analysis. *Kidney Int* 1983; 24: 626–631
4. Atkins RC, Nikolic-Paterson DJ, Song Q *et al.* Modulators of crescentic glomerulonephritis. *J Am Soc Nephrol* 1996; 7: 2271–2278
5. Ohse T, Chang AM, Pippin JW *et al.* A new function for parietal epithelial cells: a second glomerular barrier. *Am J Physiol Renal Physiol* 2009; 297: F1566–F1574
6. Quaggin SE, Kreidberg JA. Development of the renal glomerulus: good neighbors and good fences. *Development* 2008; 135: 609–620
7. Tojo A, Endou H. Intrarenal handling of proteins in rats using fractional micropuncture technique. *Am J Physiol* 1992; 263: F601–F606
8. Russo LM, Sandoval RM, McKee M *et al.* The normal kidney filters nephrotic levels of albumin retrieved by proximal tubule cells: retrieval is disrupted in nephrotic states. *Kidney Int* 2007; 71: 504–513
9. Eddy AA, Kim H, Lopez-Guisa J *et al.* Interstitial fibrosis in mice with overload proteinuria: deficiency of TIMP 1 is not protective. *Kidney Int* 2000; 58: 618–628
10. Bradley GM, Benson ES. Examination of the Urine. In: Davidson I, Henry JB, eds. *Todd-Sanford Clinical Diagnostics by Laboratory Methods*. 15th edn. Philadelphia, PA: WB Sanders,, 1974, p. 74
11. Marshall CB, Pippin JW, Krofft RD *et al.* Puromycin aminonucleoside induces oxidant-dependent DNA damage in podocytes in vitro and in vivo. *Kidney Int* 2006; 70: 1962–1973
12. Ikeda Y, Jung YO, Kim H *et al.* Exogenous bone morphogenetic protein-7 fails to attenuate renal fibrosis in rats with overload proteinuria. *Nephron Exp Nephrol* 2004; 97: e123–e135
13. Johnson AC, Yabu JM, Hanson S *et al.* Experimental glomerulopathy alters renal cortical cholesterol, SR-B1, ABCA1, and HMG CoA reductase expression. *Am J Pathol* 2003; 162: 283–291
14. Marshall CB, Krofft RD, Pippin JW *et al.* The CDK-inhibitor p21 is Pro-survival in Adriamycin(R)-Induced Podocyte Injury, in vitro and in vivo. *Am J Physiol Renal Physiol* 2010; 298: 1140–1151
15. Ohse T, Pippin JW, Vaughan MR *et al.* Establishment of conditionally immortalized mouse glomerular parietal epithelial cells in culture. *J Am Soc Nephro* 2008; 19: 1879–1890
16. Ohse T, Vaughan MR, Kopp JB *et al.* De novo expression of podocyte proteins in parietal epithelial cells during experimental glomerular disease. *Am J Physiol Renal Physiol* 2010; 298: F702–F711
17. Ohse T, Inagi R, Tanaka T *et al.* Albumin induces endoplasmic reticulum stress and apoptosis in renal proximal tubular cells. *Kidney Int* 2006; 70: 1447–1455
18. Diwakar R, Pearson AL, Colville-Nash P *et al.* The role played by endocytosis in albumin-induced secretion of TGF-β_1 by proximal tubular epithelial cells. *Am J Physiol Renal Physiol* 2007; 292: F1464–F1470
19. Gekle M, Drumm K, Mildenberger S *et al.* Inhibition of Na^+-H^+ exchange impairs receptor-mediated albumin endocytosis in renal proximal tubule-derived epithelial cells from opossum. *J Physiol* 1999; 520: 709–721
20. Hed J, Hallden G, Johansson SG *et al.* The use of fluorescence quenching in flow cytofluorometry to measure the attachment and ingestion phases in phagocytosis in peripheral blood without prior cell separation. *J Immunol Methods* 1987; 101: 119–125
21. Klippel N, Bilitewski U. Phagocytosis assay based on living Candida albicans for the detection of effects of chemicals on macrophage function. *Anal Lett* 2007; 40: 1400–1411
22. Brinkkoetter PT, Wu JS, Ohse T *et al.* p35, the non-cyclin activator of Cdk5, protects podocytes against apoptosis in vitro and in vivo. *Kidney Int* 2010; 77: 690–699
23. Hiromura K, Pippin JW, Fero ML *et al.* Modulation of apoptosis by the cyclin-dependent kinase inhibitor p27 (Kip1). *J Clin Invest* 1999; 103: 597–604
24. Logar CM, Brinkkoetter PT, Krofft RD *et al.* Darbepoetin alfa protects podocytes from apoptosis in vitro and in vivo. *Kidney Int* 2007; 72: 489–498
25. Vaughan MR, Pippin JW, Griffin SV *et al.* ATRA induces podocyte differentiation and alters nephrin and podocin expression in vitro and in vivo. *Kidney Int* 2005; 68: 133–144
26. Brinkkoetter PT, Olivier P, Wu JS *et al.* Cyclin I activates Cdk5 and regulates expression of Bcl-2 and Bcl-XL in postmitotic mouse cells. *J Clin Invest* 2009; 119: 3089–3101
27. Boehm JS, Zhao JJ, Yao J *et al.* Integrative genomic approaches identify IKBKE as a breast cancer oncogene. *Cell* 2007; 129: 1065–1079
28. Eyre J, Ioannou K, Grubb BD *et al.* Statin-sensitive endocytosis of albumin by glomerular podocytes. *Am J Physiol Renal Physiol* 2007; 292: F674–F681
29. Christensen EI, Birn H. Megalin and cubilin: synergistic endocytic receptors in renal proximal tubule. *Am J Physiol Renal Physiol* 2001; 280: F562–F573
30. Cui S, Verroust PJ, Moestrup SK *et al.* Megalin/gp330 mediates uptake of albumin in renal proximal tubule. *Am J Physiol* 1996; 271(4 Pt 2): F900-F907
31. Zhai XY, Nielsen R, Birn H *et al.* Cubilin- and megalin-mediated uptake of albumin in cultured proximal tubule cells of opossum kidney. *Kidney Int* 2000; 58: 1523–1533
32. Kerjaschki D, Farquhuar MG. Immunocytochemical localization of the Heymann nephritis antigen (GP330) in glomerular epithelial cells of normal Lewis rats. *J Exp Med* 1983; 157: 667–686
33. Odera K, Goto S, Takahashi R. Age-related change of endocytic receptors megalin and cubilin in the kidney in rats. *Biogerontology* 2007; 8: 505–515
34. Yamazaki H, Saito A, Ooi H *et al.* Differentiation-induced cultured podocytes express endocytically active megalin, a heymann nephritis antigen. *Nephron Exp Nephrol* 2004; 96: e52–e58
35. Akilesh S, Huber TB, Wu H *et al.* Podocytes use FcRn to clear IgG from the glomerular basement membrane. *Proc Natl Acad Sci U S A* 2008; 105: 967–972
36. Sarav M, Wang Y, Hack BK *et al.* Renal FcRn reclaims albumin but facilitates elimination of IgG. *J Am Soc Nephrol* 2009; 20: 1941–19–52
37. Anderson CL, Chaudhury C, Kim J *et al.* Perspective-FcRn transports albumin: relevance to immunology and medicine. *Trends Immunol* 2006; 27: 343–348
38. Wada T, Pippin JW, Nangaku M *et al.* Dexamethasone's prosurvival benefits in podocytes require extracellular signal-regulated kinase phosphorylation. *Nephron Exp Nephrol* 2008; 109: e8–e19
39. Mundel P, Reiser J. Proteinuria: an enzymatic disease of the podocyte? *Kidney Int* 2010; 77: 571–580
40. Kralik PM, Long Y, Song Y *et al.* Diabetic albuminuria is due to a small fraction of nephrons distinguished by albumin-stained tubules and glomerular adhesions. *Am J Pathol* 2009; 175: 500–509

41. Brunskill NJ, Nahorski S, Walls J. Characteristics of albumin binding to opossum kidney cells and identification of potential receptors. *Pflugers Arch* 1997; 433: 497–504
42. Haymann JP, Levraud JP, Bouet S *et al.* Characterization and localization of the neonatal Fc receptor in adult human kidney. *J Am Soc Nephrol* 2000; 11: 632–639
43. Achenbach J, Mengel M, Tossidou I *et al.* Parietal epithelia cells in the urine as a marker of disease activity in glomerular diseases. *Nephrol Dial Transplant* 2008; 23: 3138–3145
44. Dixon R, Brunskill NJ. Albumin stimulates p44/p42 extracellular-signal-regulated mitogen-activated protein kinase in opossum kidney proximal tubular cells. *Clin Sci (Lond)* 2000; 98: 295–301
45. Dixon R, Brunskill NJ. Activation of mitogenic pathways by albumin in kidney proximal tubule epithelial cells: implications for the pathophysiology of proteinuric states. *J Am Soc Nephrol* 1999; 10: 1487–1497

Received for publication: 17.6.11; Accepted in revised form: 14.7.11